Article

India's Commitments to Increase Tree and Forest Cover: Consequences for Water Supply and Agriculture Production within the Central Indian Highlands

Benjamin Clark [1],*, Ruth DeFries [1] and Jagdish Krishnaswamy [2]

1 Department of Ecology, Evolution and Environmental Biology, Columbia University, New York, NY 10027, USA; rd2402@columbia.edu
2 Suri Sehgal Centre for Biodiversity and Conservation, Ashoka Trust for Research in Ecology and the Environment (ATREE), Royal Enclave, Sriramapura, Jakkur Post, Bangalore 560 064, India; jagdish@atree.org
* Correspondence: bdc2120@columbia.edu; Tel.: +1-917-704-1458

Abstract: As part of its nationally determined contributions as well as national forest policy goals, India plans to boost tree cover to 33% of its land area. Land currently under other uses will require tree-plantations or reforestation to achieve this goal. This paper examines the effects of converting cropland to tree or forest cover in the Central India Highlands (CIH). The paper examines the impact of increased forest cover on groundwater infiltration and recharge, which are essential for sustainable Rabi (winter, non-monsoon) season irrigation and agricultural production. Field measurements of saturated hydraulic conductivity (K_{fs}) linked to hydrological modeling estimate increased forest cover impact on the CIH hydrology. K_{fs} tests in 118 sites demonstrate a significant land cover effect, with forest cover having a higher K_{fs} of 20.2 mm h^{-1} than croplands (6.7 mm h^{-1}). The spatial processes in hydrology (SPHY) model simulated forest cover from 2% to 75% and showed that each basin reacts differently, depending on the amount of agriculture under paddy. Paddy agriculture can compensate for low infiltration through increased depression storage, allowing for continuous infiltration and groundwater recharge. Expanding forest cover to 33% in the CIH would reduce groundwater recharge by 7.94 mm (−1%) when converting the average cropland and increase it by 15.38 mm (3%) if reforestation is conducted on non-paddy agriculture. Intermediate forest cover shows however shows potential for increase in net benefits.

Keywords: saturated hydraulic conductivity; depression storage; groundwater recharge; UNFCCC; forest; and tree cover

1. Introduction

India has committed to reducing greenhouse gas emission intensity under its nationally determined contributions (NDC), made at the United Nations Climate Change Conference in 2015 (COP21). To achieve this goal, India plans to create carbon sinks of 2.5 to 3 billion tons of carbon dioxide equivalents by increasing its forest and tree cover to 33% of its land area. The effort to increase tree cover up to 33% sits within the National Mission for a Green India (GIM), one of eight Missions under the National Action Plan on Climate Change (NAPCC) as well as earlier national forest policy goals. The GIM plans to increase tree cover on five million hectares of designated forest lands and forest on non-forest designated lands and improve tree cover on an additional five million hectares [1]. This effort, if achieved, would ultimately result in three to five million hectares of degraded or marginal agricultural land being converted to forest or agroforestry [2–4]. To minimize negative impacts on biodiversity and local pastoral livelihoods, conversion of natural or managed grasslands to forest will also need to be avoided [5–7]. One of the stated goals of GIM is to improve the hydrological services within the affected landscapes. Using this as a

point of departure, this paper examines the effects of converting cropland to forest cover within the Central India Highlands (CIH) to achieve 33% forest and tree cover within each river basin. It focuses on the impacts on groundwater recharge, essential for sustainable Rabi season (winter, non-monsoon season) irrigation. The CIH is selected as it contains significant forests and has rapidly increased its agriculture production and groundwater abstraction with groundwater accounting for 41% of irrigation water demand over the last decade [8]. In addition, the CIH is a hotspot for extreme precipitation events and climate change [9,10].

India ranks number ten in the world for forested area but only 120th in terms of the percentage of land area under forest [11]. The Forest Survey of India (FSI) conducted in 2019 estimates a total of 807,276 square kilometers of forest and tree cover, which makes up 24.56 percent of the land area [12]. The 2019 forest area represents an increase of 78,852 (2.4%) square kilometers over the past two decades, with the 1997 Forest Survey of India (FSI) reporting 633,397 square kilometers (19.27%) [13]. Given these estimates, India must at a minimum, increase its tree cover by 12% over the next decade, meaning adding 32,874 square kilometers per year on average. The amount of tree cover required is approximately three times the land area proposed within the GIM's stated goals. The magnitude of land cover change required to meet the COP21 commitments, if achieved, has the potential to significantly impact the hydrological cycle of the affected landscapes, with implications for both agricultural production and irrigation potential.

The infiltration-evapotranspiration trade-off hypothesis provides a framework for understanding the possible alteration of the hydrological cycle from reforestation and afforestation [14–17]. As compared to other land cover, forests have higher rates of evapotranspiration (ET) but also have higher infiltration and groundwater recharge [15,18]. The balance between these two depends on a variety of soil, geologic, and land use history, and vegetation attributes [19–21]. Through greater infiltration, groundwater recharge, and evapotranspiration, forests also reduce peak flows [17,22]. Likewise, forest compared to other land cover tends to have the lowest annual water yields [22,23]. Much of India' cultivable land is devoted to rice production in paddies where infiltration rates are slow, and ET is reduced in comparison to forest. Within the CIH 34% of the land area is devoted to paddy agriculture ranging from 18% to 73% per basin [24]. Rice is grown during the monsoon season with excess water routed through surface drainage instead of percolating to groundwater. Paddy, as a widespread cultivation practice that occupies a considerable land area within each basin, has a significant impact on the amount of groundwater recharge that can subsequently be used for groundwater-based Rabi season irrigation to support multicropping and bust agricultural production [25,26]. Consequently, forest and paddy land covers present very different dynamics in the context of the infiltration-evapotranspiration trade-off hypothesis. Conversion between these two land covers should have a substantial impact on the inter-annual dynamics of the hydrological cycle and availability of groundwater as a consequence of addressing India's COP21 commitments.

Evidence from afforestation and reforestation studies from around the world show divergent impacts on river basins. Most report a decline in basin discharge, with differences in studies between the impact on fast runoff and baseflow [27–30]. Krishnaswamy et al. 2018 [14] report neutral to positive effects of forest cover within a basin on dry-season flow, suggesting forests play a role in the temporal dynamics of streamflow. The reduction in discharge as result of planting trees is largely attributed to the increase in ET [31]. When agricultural land is converted, past cropping intensity and irrigation can have an impact on the ET changes resulting from planting trees. One exception to declining discharge was reported by Lacombe et al., 2016 where teak plantations replaced paddy agriculture in Laos. Reforestation can also alter dominant flow pathways and dampen streamflow response to precipitation events [32]. Afforestation of agricultural land within the tropics has been shown to have a dramatic impact on infiltration, with between two and four-fold increases [33]. Zhang et al. (2019) [34] report an increase in soil hydraulic conductivity in 23-year-old reforested pine, suggesting that soil properties take time to develop post tree

planting. Soil moisture has also been shown to decline after afforestation; this, however, is strongly dependent on the species, density, and phenology of the trees planted [35]. Groundwater recharge is enhanced by the condition of the forest, with plantations providing less recharge than natural forests [36] and conversely an increase in overland flow associated with degradation resulting from overuse [37]. Adjustments to basin hydrology also occur over an extended period after afforestation, with Brown et al., 2013 [27], reporting basins achieving equilibrium after 8 to 25 years and Webb and Kathuria, 2012 [28] reporting maximum streamflow reductions after 14 years. The trade-off between increased infiltration and ET resulting from reforestation can take decades to develop and may never achieve the advantageous balance of natural forest [38]. Afforestation and reforestation have complex impacts on river basin hydrology that play out over both temporal and spatial scales, making them difficult to predict [39,40].

India's total cropland area has been largely unchanged since the 1970s, at approximately 60% of the total land area [41]. To meet the ever-growing food demand of the expanding population, India has intensified its agriculture through additional growing seasons that require irrigation. Initial investments for developing irrigated croplands were predominantly in surface-irrigation schemes. In recent years, with bore wells becoming cheaper to drill, expansion of the electrical grid, and provision of pumping subsidies, many farmers have installed bore wells [42–44]. In some regions of India, this has resulted in an over-exploitation of groundwater resources and a declining water table [45]. While India has ample water resources overall [46], intra-annual variability can create temporal water stress that limits Rabi season irrigation [8].

Knowing the balance between water loss and water gain both spatially and temporally throughout the year is crucial in determining synergies or trade-offs between agricultural production and increases in forest cover for carbon sequestration. This paper seeks to answer the following:

What would be the impact of increasing forest and tree cover within the CIH to 33% of the basin area?

What type of forest and tree cover yields the maximum groundwater recharge?

Which hydrological parameters dynamics need to be considered when planning reforestation?

To answer these questions, this paper first examines the impact of land cover on field saturated hydrological conductivity (K_{fs}) in the CIH. These findings are then incorporated into a modified spatial processes in hydrology (SPHY) model for five river basins whose headwaters are within the CIH. The model is then used to simulate forest cover from 2% through 75% to identify the forest cover required to maximize groundwater recharge. The paper discusses how infiltration and depression storage interact to control groundwater recharge when reforesting paddy-based agriculture landscapes. Lastly, the paper addresses implications for agriculture production and Rabi season irrigation from groundwater sources.

2. Materials and Methods

2.1. Study Area

The study area encompasses much of the Central Highlands agro-ecological zone as defined by the National Bureau of Soil Survey and Land Use Planning [47] based on the 1992 definition [47] and consequently, we refer to the area as the Central Indian Highlands. The study area is delineated by the river basins within the CIH with outlets at gauge stations. Three out of the five selected gauge stations had adequate discharge data to calibrate the hydrological model used in this study. We chose the CIH because it is one of the few remaining forested areas in the country with potential for both reforestation and afforestation. It has rapidly increased its agricultural production and groundwater abstraction since the turn of the century and holds the headwaters of five major rivers. The study area extends from 74.76° to 83.02° East and 18.97° to 26.05° North, covering an area of 438,400 km². The area intersects with 39 districts in the states of Madhya Pradesh,

Chhattisgarh, Maharashtra, Uttar Pradesh, and Rajasthan. The five major river basins with headwaters in the study area are the Ganga, Narmada, Tapi, Godavari, and Mahanadi rivers (Figure 1). According to the European Space Agency (ESA), Climate Change Initiative 300 m Land Cover Data (CCI-LC) [48], the study area is 8.07% forest (greater than 15% canopy cover) and 87.59% agricultural lands (Table 1). The dominant form of agriculture is paddy. Dual cropping is common with rice grown during the monsoon (Kharif) period from June to November and wheat grown during the Rabi season from November to March under irrigation. There are 189 major and 309 medium irrigation schemes within the study area with a total command area of 98,736 km^2, accounting for 22% of the area. Two hundred sixty-eight reservoirs supply water to these irrigation schemes, though there has been a dramatic increase in groundwater abstraction for irrigation with an 11% increase in Madhya Pradesh from 2010 to 2017 [46,49].
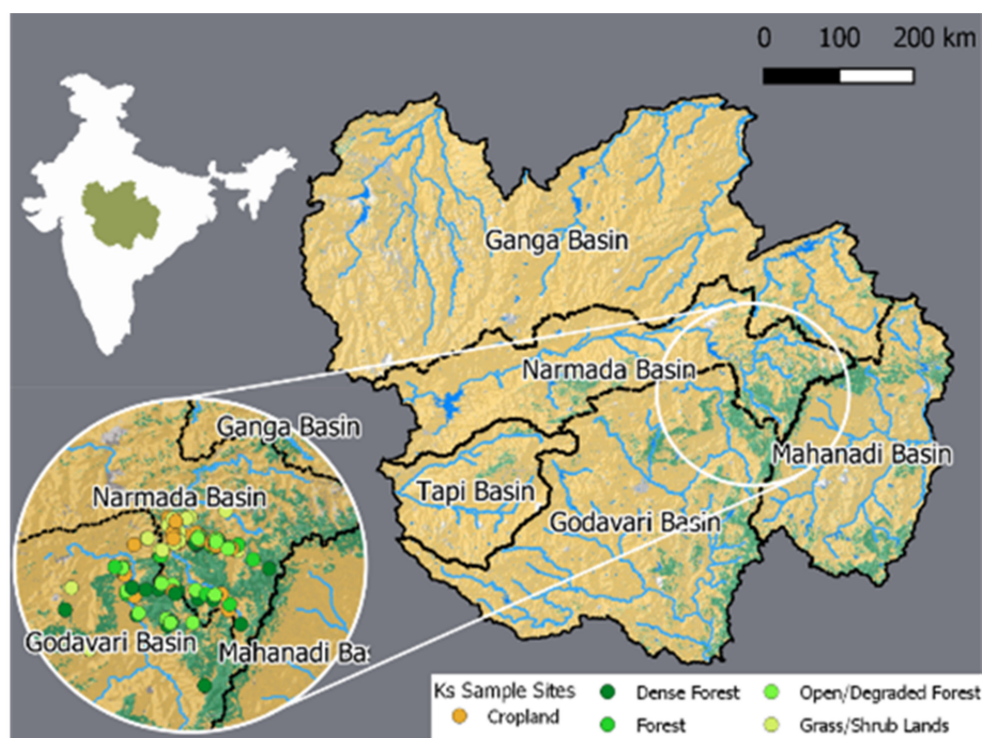
Figure 1. Central Indian highlands with the five major basins delineated. Forest cover is shown in green while agriculture is in yellow derived from the European Space Agency (ESA) Land Cover 2010 data reclassified. The inset map shows the sampling area for infiltration tests and the final sampled locations. The color of the sample locations represents the land cover.

Table 1. Basin area and forest cover from ESA Climate Change Initiative 300 m Land Cover Data (CCI) land cover data.

Basin	Area (km^2)	Forest	Cropland
Ganga	175,883	2.23%	92.22%
Godavari	107,679	12.06%	85.01%
Mahanadi	58,772	16.75%	80.55%
Narmada	66,398	11.63%	83.66%
Tapi	29,661	3.00%	92.25%
CIH	**438,393**	**8.07%**	**87.59%**

2.2. Land Cover Saturated Hydraulic Conductivity

Field data were collected to analyze the differences in field saturated hydraulic conductivity (K$_{fs}$) between broad land cover classes. Data were collected at 118 sites across

the CIH. Sites were selected based on a sampling frame that was stratified by soil order, land cover, and whether the closest Central Groundwater Board (CGWB) observation well had a positive or negative water table trending slope from 2002 to 2012. Data on soil order utilized the Soil and Land Use Survey of India detailed soil maps for Madhya Pradesh, with four soil orders present within the study area. The land cover strata contained six land cover classes: dense forest, moderate forest, open/degraded forest, grasslands, rainfed cropland, and irrigated cropland. Spatial data for grasslands and cropland were taken from the Global Irrigated Area Map data [50]. The spatial data for forest classes were developed using forest biomass data from Agarwala, M. 2015 [51]. Dense forest was defined as a forest with aboveground biomass of more than 40 Mg Ha^{-1}, moderate forest had an estimated aboveground biomass of 30 Mg Ha^{-1} to 40 Mg Ha^{-1}, and open/degraded forest had an estimated aboveground biomass less than 30 Mg Ha^{-1}. Grassland included any open area in and around the forest and land subject to grazing by village livestock. The CGWB observation wells were used to estimate temporal trends in groundwater height from 2002 to 2012 [52,53]. Theil-Sen estimator trend lines were fitted to the data for each well to estimate a positive or negative water table trend. Each well was given a five-kilometer buffer to create a sampling area. The roads within the sampling area were given 25-km buffers to create a logistically valid sampling area that was accessible by vehicle and on foot.

The sampling layers representing land cover, soil order, observation well trends, and logistically valid sampling areas were then intersected to produce sampling polygons. A three-stage random selection of sample sites was then carried out. As the intersection of the layers had the potential to create many small polygons around the same observation well, the first stage randomly selected one polygon for each stratum from each observation well to ensure the spatial distribution of the final sample. The second stage randomly selected three polygons for each stratum within the sampling frame, and the final stage randomly selected a point within the selected polygon as the sample site. Not all land cover types were present on all soil orders, and consequently, only 118 sample sites were selected. The sample sites were then visited for data collection. At each sample site, a soil sample was taken from 0 cm to 50 cm using a soil auger, the land cover (forest, grassland, cropland) was recorded and photographed, and the field saturated hydraulic conductivity measured using a DualHead Infiltrometer (Decagon Devices Inc., Pullman, DC, USA). The soil samples were used to measure texture and organic matter in an Indian Council of Agricultural Research lab using their standard methods [54]. The field data on K_{fs}, land cover and lab soil properties were collated into a dataset for analysis. An analysis of variance was carried out in R [55]. The forest sample of 47 sites included 27 sites located within teak plantations. For analysis, the study sites were reclassified as forest, teak plantation, grass/shrubland, and cropland. Only two soil texture classes were represented by the 118 sample sites resulting in the soil properties poorly representing the variables in K_{fs}. As a result, no soil properties were included in the model. The observation well water table trend had no impact on K_{fs} and was dropped from the final model. Estimated marginal means [56] were used to test significant differences in K_{fs} among land cover types implemented in the Emmeans package in R [57].

2.3. SPHY Hydrological Modeling

Landscape-scale hydrological modeling was used to link differences in land use infiltration rates to groundwater recharge and to understand the impact increased forest cover would have on the hydrology of the CIH. Simulation modeling was carried out for scenarios of forest cover at 5% intervals from 5% to 75% and included additional scenarios for 2% forest cover (approximate current minimum for some basins) and 33% forest cover (India's target COP21 NDC). The Ganga, Godavari, Mahanadi, and Narmada river basins were simulated over the period from June 2003 to June 2017. The Tapi basin had insufficient data for hydrological simulation. Hydrological modeling was conducted using a modified SPHY model [58,59]. The SPHY model was chosen for its simple parameterization, ability to be easily modified, and the availability of input data for the study area (refer to Table 2).

The SPHY model is written in Python (https://www.python.org/, accessed on 31 March 2021) and uses PCRaster (Utrecht University, Utrecht, The Netherlands) for simulation, making it easy to modify. SPHY is a gridded hydrological model with two soil layers and a groundwater layer. SPHY simulates the processes of evapotranspiration (ET), interception, through-fall, fast runoff, percolation, groundwater recharge, and baseflow on a daily time step.

For this study, the original SPHY model was modified to better represent paddy-based agriculture and more directly account for the impacts of land cover on hydrological processes than the original model. The modifications made to the model included implementing depression storage, forcing the model with observed ET time series, including a forcing time series on maximum infiltration and modifying the calculation used to estimate the soil layer K_{fs} values. Forcing the model with observed ET time series for the study period reduced the error associated with computing ET within the model. To better model paddy agriculture, the dominant crop type within the study area, depression storage was implemented in the model. Lastly, the method for computing K_{fs} was modified to account for the information learned from field observations of land cover impact on K_{fs}. To improve the model's computational efficacy, the model was converted from using PCRaster to an implementation that leveraged the graphics processing unit (GPU) to compute the model. Automated parameter estimation was carried out by implementing particle swarm optimization (PSO) [60] on the GPU.

Forcing the model with ET observed from satellites (refer to Table 2) simplified the model computations but required a daily time series of observed ET. Within the model, observed ET served as the atmospheric demand for water that had to be met from either canopy storage, depression storage, or rooting zone soil moisture. Observed ET exceeding canopy storage, depression storage, and rooting zones soil moisture represented unsatisfied demand and model error.

Table 2. Input data to the modified SPHY model used to simulate the differences in hydrology for forest cover ranging from 2% to 75% in the Central Indian Highlands.

Input Parameter	Source	(%) Spatial Resolution	(%) Temporal Resolution	Processing
Precipitation time series	PERSIANN CCS	0.04°	Daily	(%) Re-sampled to 250 m
Evapotranspiration time series	MOD16A2	500 m	8-day	(%) Re-sampled to 250 m and temporally interpolate to daily images
Leaf Area Index time series	MOD15A2H	500 m	8-day	(%) Re-sampled to 250 m and temporally interpolate to daily images
Digital Elevation Data	HydroSHED	90 m		(%) Re-sampled to 250 m, processed to delineate basins, create a slope map and D8 drainage direction map and flow accumulation map
Land Cover	ESA CCI Land cover 2010	300 m	2010	Re-sampled to 250 m with classes simplified into Forest, Shrubland, Grassland, Agriculture, Built area, Bare Soil, Water, Snow/Ice
Clay Content (%)	SoilGrids: CLYPPT	250 m		The SoilGrids Layers 1 through 7 were used to computer saturated hydraulic conductivity, saturated soil water content, water content at pF2 (field capacity), pF3 (wilting point) and pF4.2 (permanent wilting point). The 7 layers were then averaged into topsoil and subsoil layers weighted by layer thickness and land cover.
Silt Content (%)	SoilGrids: SLTPPT	250 m		
Sand Content (%)	SoilGrids: SNDPPT	250 m		
Organic Carbon Content (%)	SoilGrids: ORCDRC	250 m		
pH x 10 in H_2O	SoilGrids: PHIHOX	250 m		
Cation Exchange Capacity	SoilGrids: CECSOL	250 m		
Bulk Density	SoilGrids: BLDFIE	250 m		

As the final simulations were conducted at basin level and as such represented areas larger than most precipitation events, a time series on max infiltration was introduced to account for the spatial extent of rainstorm events. The time series was built by computing by limiting cell infiltration to Ksat and averaging the resulting data to product the max infiltration possible for the time step. In addition, a scale parameter was added to the model to further limited maximum infiltration to account for the average duration of a storm with the simulated time-stop. Depression storage was implemented in the model by creating an additional layer on top of the soil that tracked the volume of water stored on the surface. The depression storage layer was implemented as a grid with cell values representing the millimeters of depression storage. Maximum depression storage was set based on land cover. Throughfall was transferred to the depression storage layer instead of the first soil layer. After throughfall was added to depression storage, water was transferred to the first soil layer at the rate of K_{fs}. Next, any water in excess of the land cover maximum depression storage was discharged from the cell as surface runoff. Last, observed ET that was unmet by canopy storage was taken from depression storage, and the final volume of the depression storage was computed for input to the next time step within the simulation.

Land cover was incorporated into the estimation of K_{fs} based on Saxton et al., 1986 [61] pedotransfer function. The function was modified to include a land cover coefficient and forest biomass. Parameters for K_{fs} function were estimated using the field data on K_{fs} and predictors using SoilGrids (https://soilgrids.org/, accessed on 31 March 2021) data and The Global Forest Watch (https://www.globalforestwatch.org/, accessed on 31 March 2021, Washington, DC, USA) above-ground live woody biomass density database using the methodology developed by Baccini et al. 2017 [62]:

$$K_{fs} = \left(lc + (4.198 \times bm) \times \left(23.502 + 3.225 \times 24 \times e^{12.012-0.0755 \times sand} \right) \right) \times 10 \quad (1)$$

where K_{fs} is field saturated hydraulic conductivity mm day^{-1}, lc is the land cover coefficient, bm is above ground live woody biomass for forest and 0 for other land covers, and sand is percent sand in the soil. Land cover coefficients were estimated from the field data as 8.83 for forest, 3.71 for grasslands and 0 for agriculture.

The input data for the modified SPHY model included precipitation (supply), evapotranspiration (ET) (atmospheric demand), leaf area index (LAI) (time varying vegetation dynamics), soil hydrological properties, and elevation data (Table 2). The elevation data used was the HydroSHED (https://www.hydrosheds.org/, accessed on 31 March 2021, Washington, DC, USA) hydrologically conditioned elevation dataset created from Shuttle Radar Topography Mission (SRTM) data [63]. The elevation data was used to calculate the slope [64], D8 flow direction [65], and cell accumulation implemented in python package RichDEM [66]. The resulting slope, D8 flow direction, and cell accumulation layers are required for routing the water within the model and delineating the river basins. SoilGrids data [67] was used to derive the soil hydrological properties for K_{fs}, volumetric water content (VWC) at saturation, field capacity (pF 2.0), wilting point (pF 3.0), and permanent wilting point (pF 4.2) for both the topsoil and subsoil layers in the model. A number of tropical pedotransfer functions were evaluated [61,68–80] with Tomasella et al. 1998 [77] function selected to estimate VWC at field capacity, wilting point, permanent wilting point and saturation. Vereecken et al. 1989 [81] was used to estimate residual VWC. The modified model was forced with a daily time series of precipitation, LAI, and ET. The MOD16A (MODIS/Terra Net Evapotranspiration 8-Day L4 Global 500 m SIN Grid) dataset was resampled and interpolated into a daily time series [82]. The MOD16A dataset contains significant amounts of missing data. The missing data were filled using the mean cell deviance from the basin and land cover mean for the day of the year over the study period added to the basin and land cover mean for the date of the missing pixel data. This method for filling missing data maintained the spatial (land cover) and temporal variability within the data. The LAI time series, used to estimate time-varying canopy storage, was interpolated into a daily time-series using the MOD15A2 (MODIS/Terra Leaf Area Index/FPAR 8-Day L4

Global 500 m SIN Grid) dataset which was processed with missing data filled, utilizing the same methods as the ET dataset [83]. PERSIANN (Precipitation Estimation from Remotely Sensed Information using Artificial Neural Networks) CCS (Cloud Classification System) daily data were spatially resampled to create the precipitation time series for the study area [84,85]. All data were resampled to 250 m resolution and grid aligned over the study area. The model was then reduced to basin level values and simulation as a lumped model for each basin.

The modified SPHY model was calibrated using observed daily discharge at the basin outlets for all basins except the Ganga, where the discharge data are classified by the Government of India. The Water Resource Information System, Government of India (WRIS) website was used to download discharge data. The automatic calibration of seven model parameters used particle swarm optimization (PSO) [60]. The PSO optimization's objective function was the Nash–Sutcliffe (NS) efficiency index for observed versus modeled basin daily discharge. Table 3 contains a list of parameter values optimized for each basin. The Narmada basin was automatically calibrated over the period July 2003 to June 2006 and validated in the period July 2006 to June 2008. The Mahanadi basin was calibrated with discharge data from July 2003 to June 2011 and validated on the period July 2011 to June 2014. The automated PSO calibration for the Godavari basin used daily discharge data from July 2003 to June 2013 and validated on the basin daily discharge data from July 2013 to June 2017. The calibration NS scores ranged from 0.29 in the Narmada basin to 0.48 in the Godavari basin, and the validation NS scores for the basins ranged from −1.05 (Mahanadi) to 0.36 (Godavari) (Figure 2). The calibrated parameters for the Godavari basin within the CIH were used for the CIH portion of the Ganga basin simulations because it could not be directly calibrated. The Godavari soil properties were the closest match to the Ganga of the three calibrated basins. The calibrated scenarios were simulated daily over the period from June 2003 to June 2017. The first two years of the simulation were not included in the results to allows for burn-in and the simulation to stabilize.
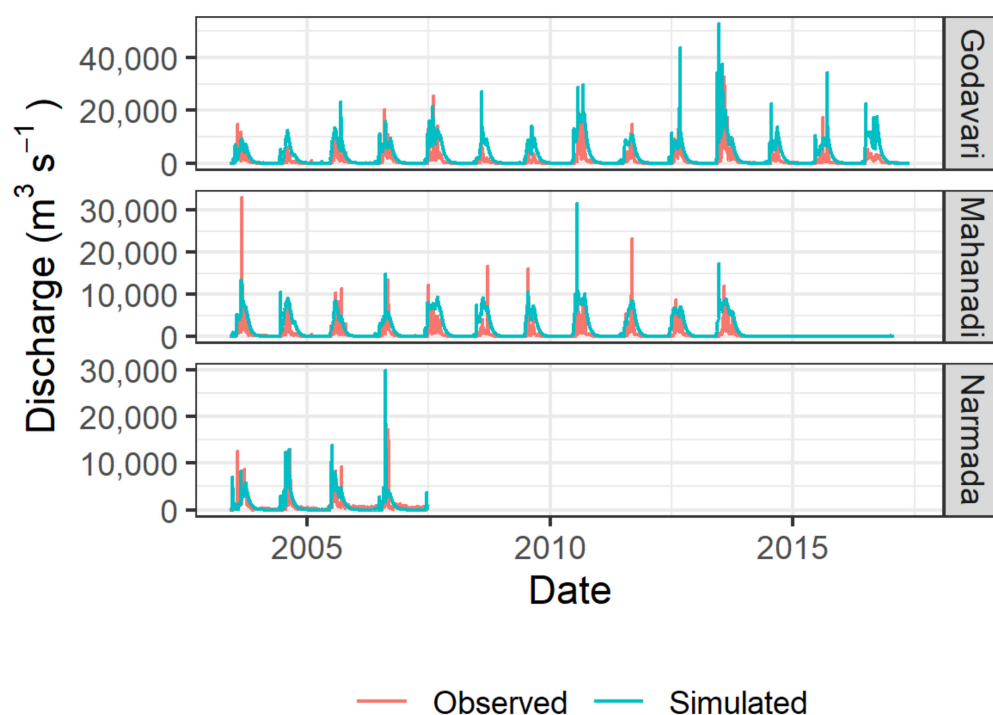
Figure 2. Observed versus daily simulated discharge for the three river basins with available discharge data for the study period.

Table 3. Result of the particle swarm optimization. Each of the three basins was optimized individually using the Nash–Sutcliffe efficiency index as the objective function computed from daily simulations of basin discharge.

	Nash Sutcliffe Efficiency Index		
Basin	Calibration	Validation	Full Period
Godavari	0.48	0.36	0.43
Mahanadi	0.35	−1.05	0.09
Narmada	0.29	−1.19	0.18

2.4. Forest Cover Scenarios

Two different pathways to reforesting and/or afforesting were simulated to determine the impact of forest cover on the hydrology of the CIH. The first pathway used mean basin values and represented an unplanned, opportunistic approach to implementing forest cover increase. The second pathway attempted to optimize groundwater recharge by preferentially converting non-paddy agriculture land. Within each pathway, seventeen levels of forest cover were implemented, starting at 2%, then in 5% increments from 5% to 75%, and an additional level at the targeted 33% forest cover within each river basin in the CIH. The scenarios were constructed by computing from mean basin SPHY model input parameter values for each land cover type at 100% basin coverage and then calculated as percent weighted averages by the percentage of each land cover within the given forest cover level. The implementation of the groundwater recharge optimized pathway used district-level agriculture statistics to estimate the area of paddy and non-paddy agriculture within each basin and adjusted depression storage for each basin by first converting non-paddy to forest. The simulated pathways represent the final hydrological equilibrium after reforestation and do not account for the period where soil parameters are altered by the growth of the trees. The 34 scenarios representing two different approaches to reforesting or afforesting, and forest cover levels were then simulated over the period 2003 to 2017 using the calibrated SPHY model to yield the results on the impact of forest cover on hydrological fluxes within the CIH river basins.

The primary changes to the model parameters over the different forest cover scenarios were the amount of depression storage within each basin, and the rate of K_{fs} (Figure 3). K_{fs} remained the same between the two pathways but varied by the amount of forest cover. The Mahanadi basin had the least change in K_{fs} of 144 mm day^{-1} from 2% to 75% forest cover, while the Narmada had the greatest change of 131 mm day^{-1} over the full range of simulated forest cover. The basin mean pathway had reductions in depression storage from 2% to 75% forest cover across all basins ranging from −9 mm to −47 mm, depending on the amount of paddy agriculture in each basin. The optimized groundwater pathway had reduced changes in depression storage ranging from 2 mm to −35 mm and was able to maintain more depression storage while increasing forest cover by preferentially converting non-paddy agriculture land. The interactions between depression storage and K_{fs} within the SPHY model exerted significant control on groundwater recharge dynamics.
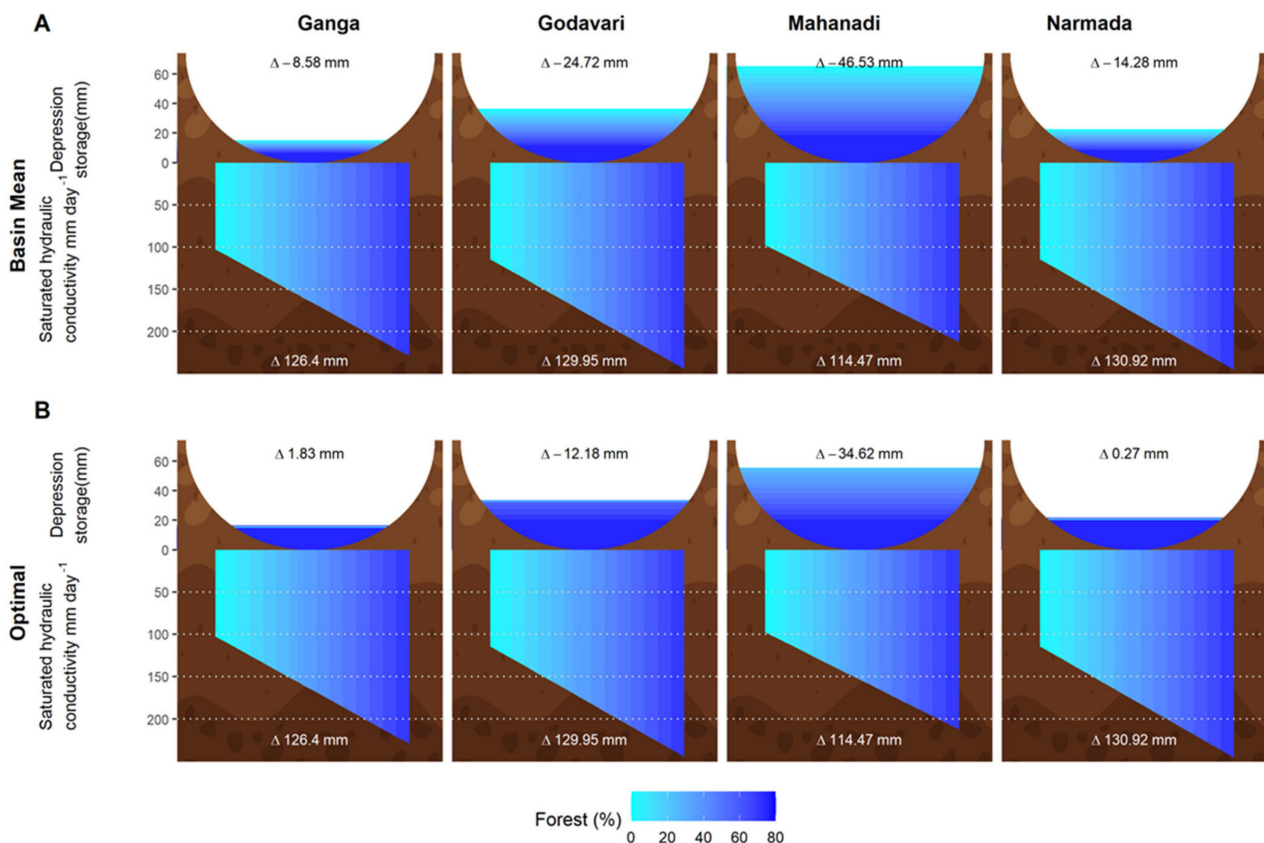
Figure 3. Basin hydrological flux changes over the range of forest cover from 2% to 75%. Evapotranspiration (**A**) shows a linear increase as forest cover increases. The basin mean pathway to increase forest cover (**B**) shows a complex curved relationship of groundwater recharge with increase forest cover. All basins have maximum groundwater recharge near to the current forest cover. Graphs show groundwater recharge for the groundwater recharge optimized pathway. The optimized pathway demonstrates that it is possible to achieve increases to groundwater recharge with increased forest cover at the basin scale depending on the land converted to forest.

3. Results

3.1. Land Cover Saturated Hydraulic Conductivity

The results of the analysis of variance of K_{fs} are significant $F_{(3, 105)} = 2.815$, $p = 0.043$ for land cover. There are significant estimated marginal means (EMM) differences between treed land cover (forest and plantations) and non-treed (grass/shrubland and cropland). Forest land cover had an EMM K_{fs} of 20.2 mm/h^{-1}, while cropland had the lowest EMM K_{fs} of 6.7 mm/h^{-1} (Figure 4). Teak plantations had the highest EMM K_{fs} of 23.2 mm/h^{-1} but were not significantly different from natural forest cover. Grass/Shrubland K_{fs} has a lot of overlap with croplands with a EMM Kfs of 7.0 mm/h^{-1}. Above-ground biomass was also a significant predictor in the model for forested areas, suggesting that forest quality can have an impact on K_{fs}. To put the results in context, hourly precipitation intensity computed from the Jabalpur weather station in the Integrated Surface Dataset reveals that median precipitation intensity exceeds forest K_{fs} approximately 46% of the time compared to cropland where median precipitation intensity exceeds K_{fs} about 67% of the time.
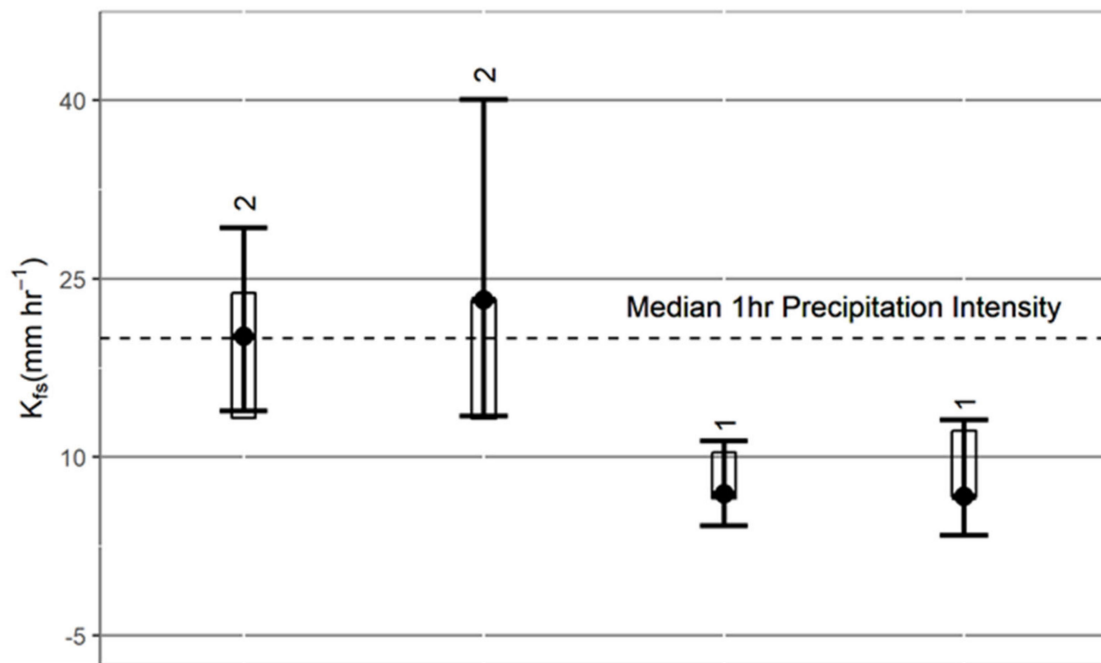
Figure 4. Estimated marginal means for the different land cover types. Error bars represent 95% confidence intervals. Crossbars that overlap are not significantly different. *p* values adjusted using the Tukey method for comparing a family of four estimates. Significance level used was alpha = 0.05. Plantation refers to teak plantations. The median 1 h precipitation intensity for the Jabalpur weather station from the Surface Integrated Dataset it plotted to assist interpretation.

3.2. Hydrological Modeling

The results from the modified SPHY model simulating forest cover increases from 2% to 75% of the basin area show considerable differences between the two reforestation/afforestation pathways. Across the CIH, the basin mean pathway reaches maximum groundwater recharge at ~10% forest cover with a total groundwater recharge of 624 mm (Figure 5A). The maximum groundwater recharge requires only a 1.5% increase in forest cover from the current landscape level of 8.5%, and this represents only a 0.06 mm increase in groundwater recharge. Achieving the targeted 33% forest cover on the basin mean pathway would result in a −7.94 mm of groundwater recharge. When accounting for the increased losses to ET with increased forest cover, the maximum groundwater recharge minus ET occurs at 2% forest cover with a balance of 177 mm (Figure 5B). The difference compared to the current forest cover would be a loss of ~5.5% of forest cover with an increase of 1.5 mm of ET compensated groundwater recharge. Similarly, achieving the target or 33% forest cover across the landscape would result in a loss of 14 mm of water from the current forest cover after accounting for the increase in ET. The basin mean pathway groundwater recharge is almost optimized as current forest cover levels, and forest cover has already exceeded the optimal when accounting for the increase in ET.

In contrast, the optimized pathway achieves maximum groundwater recharge of 640 mm at ~55% forest cover (Figure 5C). Compared to the current forest cover, there is an increase of 19 mm of groundwater recharge and 15 mm at 33% forest cover. When compensating for ET the maximum occurs at 40% forest cover with an increase of 10 mm for a total of 185 mm compared to the current forest cover of 179 mm (Figure 5D). 33% of forest cover yields a similar increase of 9 mm. The optimized pathway yields an additional 7 mm of ET compensated groundwater recharge when maximized compared with the basin mean and 38% more forest cover across the entire landscape. At 33% forest cover, the two pathways are even more divergent with a difference of 22 mm of ET compensated groundwater recharge. The two pathways emphasize the importance of good planning

and an understanding of the hydrological impacts of reforesting or afforesting at the landscape scale.

The four river basins modeled showed similar outcomes for the basin mean pathway but differed for the groundwater recharge optimized pathway. For the basin mean, all four basins are quite close to their maximum groundwater recharge at current forest cover (Figure 6E–H). Only the Narmada would benefit from a marginal increase in forest cover (Figure 6H). All four show a loss in groundwater recharge at the target of 33% forest cover ranging from −12 mm in the Godavari to −2 mm in the Narmada. The optimized pathway shows the potential to increase groundwater recharge in all four basins ranging from 1 mm in the Mahanadi basin to 46 mm increase in the Narmada basin (Figure 6I–L). Only the Mahanadi maximizes its groundwater recharge before 33% forest cover at ~25%. The other basins maximize groundwater recharge at 55%, 70%, and 75% for the Godavari, Narmada, and Ganga, respectively. The groundwater recharge increase, from current to 33% forest cover, is −5 mm for the Mahanadi basin to 27 mm for the Ganga basin. The difference between the two pathways and between the basins can be explained by the difference in depression storage over the range of forest cover (Figure 6).
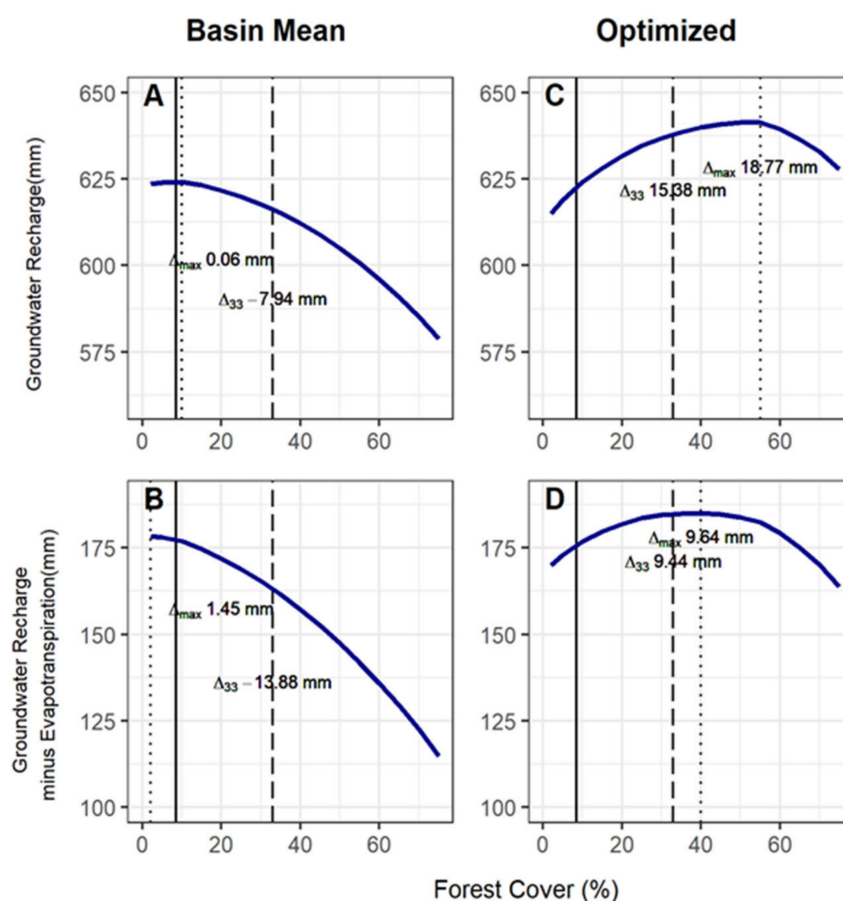
Figure 5. Central Indian Highland's groundwater recharge over the range of forest cover from 2% to 75% of the landscape. Graph (**A**) represents the groundwater recharge for the basin mean pathway for increasing forest cover while Graph (**C**) represents groundwater recharge optimized pathway to increasing forest cover. Graphs (**B,D**) subtract the increase in evapotranspiration from groundwater recharge to represent water losses from the landscape because of increasing forest cover for the basin mean pathways (**B**) and groundwater recharge optimized pathway (**D**). Δ_{33} indicates the change from current forest cover (solid vertical line) to forest cover at 33% (dashed vertical line) while Δ_{max} indicates the change from current forest cover to the maximum (dotted vertical line).
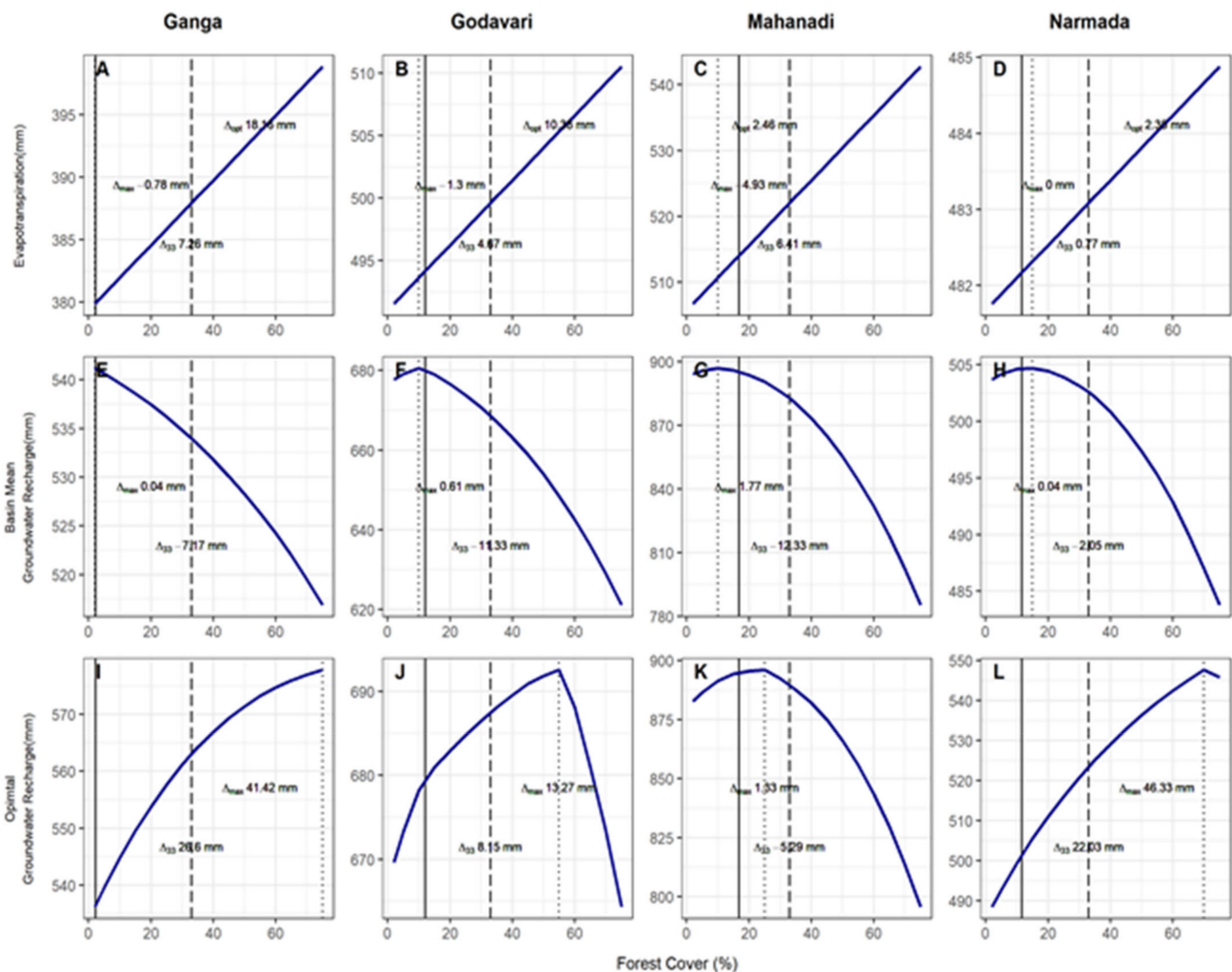
Figure 6. Basin hydrological flux changes over the range of forest cover from 2% to 75%. Evapotranspiration (**A–D**) shows a linear increase as forest cover increases. The basin mean pathway to increase forest cover (**E–H**) shows a complex curved relationship of groundwater recharge with increase forest cover. All basins have maximum groundwater recharge near to the current forest cover. Graphs (**I–L**) show groundwater recharge for the groundwater recharge optimized pathway. The optimized pathway demonstrates that it is possible to achieve increases to groundwater recharge with increased forest cover at the basin scale depending on the land converted to forest.

4. Discussion

India's NDC at COP21 of reducing its greenhouse gas emissions, partly by increasing tree cover, will require balancing the loss of agricultural land with increased production through intensification and irrigation of Rabi season crops to maintain the nation's food production. Previous studies have shown that increased use of groundwater for irrigation in Northern India is not sustainable due to rapidly falling water tables [45]. The CIH over the last decade has seen a substantial increase in groundwater abstraction for irrigation which is estimated to account for approximately 41% of irrigation water withdrawals [8] and requires 1.2 ha of land to recharge the irrigation water demand for one hectare of multi-cropping agricultural land. The infiltration-evapotranspiration trade-off hypothesis would suggest that increasing forest cover should help with groundwater recharge at the expense of increased ET. Forests are also linked to reduced basin water yield [23,86], which is currently essential to maintaining surface water irrigation schemes within the region. Much of the reduced water yield can be accounted for by the increase in ET with the remainder resulting from reductions in peak flows generated from surface runoff, which can be important in reducing the frequency and intensity of destructive floods [27,87,88].

Forest cover can also increase baseflow, resulting in healthier river systems and delayed discharge [87]. Forest and tree cover can also feed-back into and interact with the atmosphere to reduce temperatures and recycle ET into increased rainfall at the landscape or regional scale, as highlighted by Noordwijk 2018 [89] in his forest-water paradigms and also demonstrated for the Western Ghats where forest ET contribution to rainfall in dry parts of Southern India is indicated [90]. Reduced peak flows and increased baseflows would also fill reservoirs more slowly and make water available for Rabi season irrigation. Consequently, increasing forest cover within the CIH has complex hydrological interactions related to sustaining groundwater-irrigated agricultural production within the region.

The hydrological modeling carried out in this study, supported with the field data collection on K_{fs}, sheds light on how increased forest cover might impact the hydrological cycle and the consequences for irrigated food production within the CIH. The field data on K_{fs} shows a three-fold difference between forest K_{fs} and cropping K_{fs}, irrespective of soil type, with no difference between teak plantations and natural forests. Forest K_{fs} roughly matches the median rainfall intensity, while agriculture K_{fs} is likely to generate runoff during two thirds of the rainfall events. Paddy rice is the dominant form of agriculture and covers a large percentage (20% to 90% of the agricultural land area) and consequently important for recharging groundwater. Paddy differs from forest and other agriculture land cover due to its large depression storage. The results of the hydrological modeling show that the current landscape, dominated by paddy agriculture, has large volumes of depression storage but low infiltration rates. In comparison, increasing forest cover would greatly reduce depression storage while improving infiltration rates. The hydrological modeling shows that increased depression storage can largely cancel out the increase in infiltration rates when converting paddy agriculture to forest [91]. Depression storage allows water to infiltrate on a continual basis, whereas with the lack of depression storage, the process of infiltration predominantly occurs during rainfall events. The depth of water in paddies acts as a buffer that over time allows significant amounts of water to infiltrate even though the rate is slow, while forests primarily rely on fast infiltration during storm events. Converting non-paddy agricultural land, which has low infiltration and depression storage, to forest results in optimal groundwater recharge.

The two pathways to reforestation or afforestation simulated in the hydrological modeling within the basins of the CIH demonstrate the need to think carefully as to where to plant trees to increase groundwater recharge. The basin mean approach demonstrates that a lack of strategic planning would yield no hydrological benefits and a decrease in groundwater recharge while also losing agriculture production. On the other hand, the groundwater recharge optimized pathway demonstrates that planting trees in the non-forested land cover other than paddy would yield considerably more groundwater recharge with intermediate forest cover showing gains in potential to increase net benefits. Both pathways result in similar losses of water to ET. The two pathways also differ in the amount of surface runoff, with the basin mean pathway increase surface runoff by ~36 mm while the groundwater optimized pathway reduces it by ~25 mm. Reducing surface runoff would have a positive effect on reducing flooding and siltation of surface water bodies. The trade-off for improved groundwater recharge of optimized increased forest cover would be the reduction in overall discharge and increase in ET. Rabi season irrigation from groundwater sources would benefit from the increase in groundwater recharge, while the increase in ET and diminished discharge would have little impact.

Planning forest cover increases in paddy agriculture areas requires balancing losses of depression storage with an increase in infiltration rates to achieve beneficial hydrological dynamics [92]. The impact of the method used to reforest paddy on the infiltration rate and depression storage will also influence the time it takes for the site to reach a new hydrological equilibrium. Methods that focus on restoring hydrological function by increasing infiltration should reduce the time to the new equilibrium. A loss in depression storage as a consequence of converting paddy to forest will result in a reduction of groundwater recharge until the forest can improve the infiltration and restore the groundwater recharge.

To increase tree cover on paddy while minimizing negative impacts on groundwater recharge, infiltration rates in paddy would need to increase to compensate for the loss of depression storage.

This study focuses on the impact of forest cover on infiltration and its linkages to groundwater recharge at the landscape scale. The analysis provides insight into the trade-off between infiltration rate and depression storage in paddy agricultural landscape, but it has not addressed where on the landscape reforestation or afforestation could optimize groundwater recharge. Likewise, this study has not looked at the influence of forest cover on other hydrological parameters. Spracklen et al. 2012 [93] included India as one regions of the world where forest cover has the potential to increase rainfall. Additionally, the model does not address the dynamics of the period after reforestation when soil properties are being altered by tree and understory growth with increasing infiltration, balanced with the increased ET. This period may represent a very different balance from the result presented here, as ET is likely to develop faster than the change in infiltration, especially in converted paddy. There are potentially multiple synergistic benefits from increasing forest cover in the CIH that would promote better ecological function and sustainable agriculture at the landscape scale.

While India made ambitious commitments at COP21 in setting a 33% tree cover target, current land use poses a significant challenge to achieving the aims GIM. The results of this study indicate that the hydrological aims of the GIM would be promoted by increasing forest cover, but only if balanced with losses of depression storage by preferentially retaining agricultural land with maximum depression storage such as paddy. The cost to cropland would be high, but the improved hydraulic dynamics at the landscape scale from well-planned reforestation or afforestation would help improve the sustainability of Rabi irrigation. Alternatively, there are advantages to crop diversification away from paddy to alternative cereals such as millet, sorghum and maize from both sustainability and nutritional perspectives [94]. Here the focus should be on soil management and cultivation methods that increase either or both depression storage and infiltration rates on non-paddy cropland and non-forested lands. Agroforestry systems would also be explored as a method for increasing tree cover while promoting agricultural production [95–98]. Such approaches would increase nutritional output while reducing irrigation water demand and would also have a large impact on improving groundwater recharge at the landscape level. There is potential for increased tree and forest cover to boost both food production and water availability. More research is needed to better understand the dynamics of reforestation and afforestation within paddy agriculture landscapes like the CIH.

5. Conclusions

In conclusion, to address this paper's key questions, increasing forest and tree cover within the CIH can have a positive impact on groundwater recharge if strategically planned. Increased infiltration from trees (offset by loss from evapotranspiration) might not compensate for the loss of groundwater recharge resulting from a decrease in depression storage if trees replace paddy agriculture. Increasing tree cover on unforested non-paddy land, on the other hand, would have a net benefit for groundwater recharge and increase water availability for Rabi crops. This study shows that careful planning is needed when increasing forest and tree cover within paddy agriculture landscapes to achieve carbon sequestration goals without negative impacts on the hydrology and possibly intensifying inter-annual water stress within the landscape. Intermediate or moderate tree densities have the potential to increase net benefits. Balancing the loss of depression storage with the eventual increase in infiltration and increase in ET resulting from reforestation will determine the success of India's NDC efforts to sequester carbon while simultaneously improving the hydrology of the landscape.

Author Contributions: Conceptualization, R.D.; software, B.C.; formal analysis, B.C.; field research and data collection, B.C., R.D. and J.K.; writing—original draft preparation, B.C.; writing—review and editing, R.D. and J.K. All authors have read and agreed to the published version of the manuscript.

References

1. Ministry of Environment and Forests, Government of India: National Mission for a Green India. Available online: http://www.jkforest.gov.in/pdf/gim/GIM_Mission-Document-1.pdf (accessed on 31 March 2021).
2. Singh, V.P.; Sinha, R.B.; Nayak, D.; Neufeldt, H.; van Noordwijk, M.; Rizvi, J. *The National Agroforestry Policy of India: Experiential Learning in Development and Delivery Phases*; ICRAF Working Paper No. 240; World Agroforestry Centre: New Delhi, India, 2016; pp. 1–40. Available online: http://apps.worldagroforestry.org/downloads/Publications/PDFS/WP16143.pdf (accessed on 31 March 2021).
3. Dhyani, S.K. National Agroforestry Policy 2014 and the need for area estimation under agroforestry. *Curr. Sci.* **2014**, *107*, 9–10.
4. Chavan, S.B.; Keerthika, A.; Dhyani, S.K.; Handa, A.K.; Newaj, R.; Rajarajan, K. National Agroforestry Policy in India, a low hanging fruit. *Curr. Sci.* **2015**, *108*, 1826–1834.
5. Bremer, L.L.; Farley, K.A. Does plantation forestry restore biodiversity or create green deserts? A synthesis of the effects of land-use transitions on plant species richness. *Biodivers. Conserv.* **2010**, *19*, 3893–3915.
6. Iezzi, M.; De Angelo, C.; Di Bitetti, M. Tree plantations replacing natural grasslands in high biodiversity areas: How do they affect the mammal assemblage? *Ecol. Manag.* **2020**, *473*, 118303. [CrossRef]
7. Bond, W.J.; Parr, C.L. Beyond the forest edge, Ecology, diversity and conservation of the grassy biomes. *Biol. Conserv.* **2010**, *143*, 2395–2404. [CrossRef]
8. Clark, B.; DeFries, R.; Krishnaswamy, J. Intra-annual dynamics of water stress in the central Indian Highlands from 2002 to 2012. *Reg. Environ. Chang.* **2016**, *16*, 83–95. [CrossRef]
9. Roxy, M.K.; Ghosh, S.; Pathak, A.; Athulya, R.; Mujumdar, M.; Murtugudde, R.; Terray, P.; Majeevan, M. A threefold rise in widespread extreme rain events over central India. *Nat. Commun.* **2017**, *8*, 708. [CrossRef] [PubMed]
10. Goswami, B.N.; Venugopal, V.; Sengupta, D.; Madhusoodanan, M.S.; Xavier, P.K. Increasing Trend of Extreme Rain Events Over India in a Warming Environment. *Science* **2006**, *314*, 1442–1445. [CrossRef] [PubMed]
11. The World Bank. *World Development Indicators, Rural Environment and Land Use*; The World Bank: Washington, DC, USA, 2018.
12. Ministry of Environment and Forests. *Forest Survey of India*; Ministry of Environment and Forests: Dehra Dun, India, 2019.
13. Ministry of Environment and Forests. *Forest Survey of India*; Ministry of Environment and Forests: Dehra Dun, India, 1997.
14. Krishnaswamy, J.; Kelkar, N.; Birkel, C. Positive and neutral effects of forest cover on dry-season stream flow in Costa Rica identified from Bayesian regression models with informative prior distributions. *Hydrol. Process.* **2018**, *32*, 3604–3614. [CrossRef]
15. Krishnaswamy, J.; Bonell, M.; Venkatesh, B.; Purandara, B.K.; Rakesh, K.N.; Lele, S.; Kiran, M.C.; Reddy, V.; Badiger, S. The groundwater recharge response and hydrologic services of tropical humid forest ecosystems to use and reforestation: Support for the "infiltration-evapotranspiration trade-off hypothesis". *J. Hydrol.* **2013**, *498*, 191–209. [CrossRef]
16. Maréchal, J.-C.; Varma, M.R.; Riotte, J.; Vouillamoz, J.-M.; Kumar, M.M.; Ruiz, L.; Sekhar, M.; Braun, J.-J. Indirect and direct recharges in a tropical forested watershed: Mule Hole, India. *J. Hydrol.* **2009**, *364*, 272–284. [CrossRef]
17. Bruijnzeel, L.A. Hydrological functions of tropical forests, not seeing the soil for the trees? *Agric. Ecosyst. Environ.* **2004**, *104*, 185–228. [CrossRef]
18. Krishnaswamy, J.; Bonell, M.; Venkatesh, B.; Purandara, B.K.; Lele, S.; Kiran, M.; Reddy, V.; Badiger, S.; Rakesh, K. The rain–runoff response of tropical humid forest ecosystems to use and reforestation in the Western Ghats of India. *J. Hydrol.* **2012**, *472–473*, 216–237. [CrossRef]
19. Peña-Arancibia, J.L.; Bruijnzeel, L.A.; Mulligan, M.; van Dijk, A.I. Forests as 'sponges' and 'pumps': Assessing the impact of deforestation on dry-season flows across the tropics. *J. Hydrol.* **2019**, *574*, 946–963. [CrossRef]

20. International Union of Forest Research Organizations (IUFRO). *Forest and Water on a Changing Planet: Vulnerability, Adaptation and Governance Opportunities*; A Global Assessment Report IUFRO World Series Volume 38; Creed, I.F., van Noordwijk, M., Eds.; International Union of Forest Research Organizations (IUFRO): Vienna, Austria, 2018; pp. 1–190. ISBN 978-3-902762-95-5.

21. Creed, I.F.; Jones, J.A.; Archer, E.; Claassen, M.; Ellison, D.; McNulty, S.G.; Van Noordwijk, M.; Vira, B.; Wei, X.; Bishop, K.; et al. Managing Forests for Both Downstream and Downwind Water. *Front. Glob. Chang.* **2019**, *2*, 2. [CrossRef]

22. Roa-García, M.C.; Brown, S.; Schreier, H.; Lavkulich, L.M. The role of land use and soils in regulating water flow in small headwater catchments of the Andes. *Water Resour. Res.* **2011**, *47*, 47. [CrossRef]

23. Brown, A.E.; Zhang, L.; McMahon, T.A.; Western, A.W.; Vertessy, R.A. A review of paired catchment studies for determining changes in water yield resulting from alterations in vegetation. *J. Hydrol.* **2005**, *310*, 28–61. [CrossRef]

24. Task Committee on Revision of Manual 70. *Evaporation, Evapotranspiration, and Irrigation Water Requirements*; Jensen, M.E., Allen, R.G., Eds.; Society of Civil Engineers: Reston, VA, USA, 2015.

25. Liu, C.-W.; Tan, C.-H.; Huang, C.-C. Determination of the magnitudes and values for groundwater recharge from Taiwan's paddy field. *Paddy Water Environ.* **2005**, *3*, 121–126. [CrossRef]

26. Tanaka, K.; Funakoshi, Y.; Hokamura, T.; Yamada, F. The role of paddy rice in recharging urban groundwater in the Shira River Basin. *Paddy Water Environ.* **2010**, *8*, 217–226. [CrossRef]

27. Brown, A.E.; Western, A.W.; McMahon, T.A.; Zhang, L. Impact of forest cover changes on annual streamflow and flow duration curves. *J. Hydrol.* **2013**, *483*, 39–50. [CrossRef]

28. Webb, A.A.; Kathuria, A. Response of streamflow to afforestation and thinning at Red Hill, Murray Darling Basin, Australia. *J. Hydrol.* **2012**, *412–413*, 133–140. [CrossRef]

29. Dung, B.X.; Gomi, T.; Miyata, S.; Sidle, R.C.; Kosugi, K.; Onda, Y. Runoff responses to forest thinning at plot and catchment scales in a headwater catchment draining Japanese cypress forest. *J. Hydrol.* **2012**, *444–445*, 51–62. [CrossRef]

30. Huang, X.-D.; Shi, Z.-H.; Fang, N.-F.; Li, X. Influences of Land Use Change on Baseflow in Mountainous Watersheds. *Forests* **2016**, *7*, 16. [CrossRef]

31. Trabucco, A.; Zomer, R.J.; Bossio, D.A.; van Straaten, O.; Verchot, L.V. Climate change mitigation through afforestation/reforestation: A global analysis of hydrologic impacts with four case studies. *Agric. Ecosyst. Environ.* **2008**, *126*, 81–97. [CrossRef]

32. Van Meerveld, H.J.; Zhang, J.; Tripoli, R.; Bruijnzeel, L.A. Effects of Reforestation of a Degraded Imperata Grassland on Dominant Flow Pathways and Streamflow Responses in Leyte, the Philippines. *Water Resour. Res.* **2019**, *55*, 4128–4148. [CrossRef]

33. Ilstedt, U.; Malmer, A.; Verbeeten, E.; Murdiyarso, D. The effect of afforestation on water infiltration in the tropics: A systematic review and meta-analysis. *Ecol. Manag.* **2007**, *251*, 45–51. [CrossRef]

34. Zhang, J.; Bruijnzeel, L.A.; Quiñones, C.M.; Tripoli, R.; Asio, V.B.; Van Meerveld, H.J. Soil physical characteristics of a degraded tropical grassland and a 'reforest', Implications for runoff generation. *Geoderma* **2019**, *333*, 163–177. [CrossRef]

35. Yao, Y.; Wang, X.; Zeng, Z.; Liu, Y.; Peng, S.; Zhu, Z.; Piao, S. The Effect of Afforestation on Soil Moisture Content in Northeastern China. *PLoS ONE* **2016**, *11*, e0160776. [CrossRef] [PubMed]

36. Patil, N.G.; Tiwary, P.; Pal, D.K.; Bhattacharyya, T.; Sarkar, D.; Mandal, C.; Mandal, D.K.; Chandran, P.; Ray, S.K.; Prasad, J.; et al. Soil Water Retention Characteristics of Black Soils of India and Pedotransfer Functions Using Different Approaches. *J. Irrig. Drain. Eng.* **2013**, *139*, 313–324. [CrossRef]

37. Ghimire, C.P.; Bonell, M.; Bruijnzeel, L.A.; Coles, N.A.; Lubczynski, M.W. Reforesting severely degraded grassland in the Lesser Himalaya of Nepal: Effects on soil hydraulic conductivity and overland flow production. *J. Geophys. Res. Earth Surf.* **2013**, *118*, 2528–2545. [CrossRef]

38. Ghimire, C.P.; Bruijnzeel, L.A.; Lubczynski, M.W.; Bonell, M. Negative trade-off between changes in vegetation water use and infiltration recovery after reforesting degraded pasture land in the Nepalese Lesser Himalaya. *Hydrol. Earth Syst. Sci.* **2014**, *18*, 4933–4949. [CrossRef]

39. Zhang, M.; Liu, N.; Harper, R.; Li, Q.; Liu, K.; Wei, X.; Ning, D.; Hou, Y.; Liu, S. A global review on hydrological responses to forest change across multiple spatial scales: Importance of scale, climate, forest type and hydrological regime. *J. Hydrol.* **2017**, *546*, 44–59. [CrossRef]

40. Ilstedt, U.; Tobella, A.B.; Bazié, H.R.; Bayala, J.; Verbeeten, E.; Nyberg, G.; Sanou, J.; Benegas, L.; Murdiyarso, D.; Laudon, H.; et al. Intermediate tree cover can maximize groundwater recharge in the seasonally dry tropics. *Sci. Rep.* **2016**, *6*, 21930. [CrossRef]

41. The World Bank. World Development Indicators, 2018. Agricultural Land (% of Land Area). Available online: https://data.worldbank.org/indicator/AG.LND.AGRI.ZS (accessed on 31 March 2021).

42. Kumar, M.D.; Scott, C.A.; Singh, O.P. Inducing the shift from flat-rate or free agricultural power to metered supply, Implications for groundwater depletion and power sector viability in India. *J. Hydrol.* **2011**, *409*, 382–394. [CrossRef]

43. Shiferaw, B.; Reddy, V.; Wani, S. Watershed externalities, shifting cropping patterns and groundwater depletion in Indian semi-arid villages, The effect of alternative water pricing policies. *Ecol. Econ.* **2008**, *67*, 327–340. [CrossRef]

44. Sishodia, R.P.; Shukla, S.; Graham, W.D.; Wani, S.P.; Jones, J.W.; Heaney, J. Current and future groundwater withdrawals: Effects, management and energy policy options for a semi-arid Indian watershed. *Adv. Water Resour.* **2017**, *110*, 459–475. [CrossRef]

45. Rodell, M.; Velicogna, I.; Famiglietti, J.S. Satellite-based estimates of groundwater depletion in India. *Nature* **2009**, *460*, 999–1002. [CrossRef] [PubMed]

46. Central Ground Water Board. *Ground Water Year Book—India 2016–2017*; Central Ground Water Board Ministry of Water Resources Government of India: Faridabad, India, 2017.

47. Mandal, D.K.; Mandal, C.; Singh, S.K. Delineating Agro-Ecological Regions. Available online: https://www.nbsslup.in/assets/uploads/clinks/Delineating%20Agro-Ecological%20Regions.pdf (accessed on 31 March 2021).

48. Defourny, P.; Kirches, G.; Brockmann, C.; Boettcher, M.; Peters, M.; Bontemps, S.; Lamarche, C.; Schlerf, M.; Santoro, M. *Land Cover CCI, Product User Guide Version 2, 2016*; UCL-Geomatics: London, UK, 2016.

49. Central Ground Water Board Ministry of Water Resources Government of India. *Ground Water Scenario of India 2009–2010*; Central Ground Water Board Ministry of Water Resources Government of India: Faridabad, India, 2010; pp. 1–46.

50. Thenkabail, P.S.; Biradar, C.M.; Noojipady, P.; Dheeravath, V.; Li, Y.; Velpuri, M.; Gumma, M.; Gangalakunta, O.R.P.; Turral, H.; Cai, X.; et al. Global irrigated area map (GIAM), derived from remote sensing, for the end of the last millennium. *Int. J. Remote Sens.* **2009**, *30*, 3679–3733. [CrossRef]

51. Agarwala, M. Forest Degradation and Governance in Central India, Evidence from Ecology, Remote Sensing and Political Ecology. Ph.D. Thesis, Columbia University, New York, NY, USA, 2015.

52. Shekhar, S.; Kumar, S.; Densmore, A.L.; Van Dijk, W.M.; Sinha, R.; Kumar, M.; Joshi, S.K.; Rai, S.P.; Kumar, D. Modelling water levels of northwestern India in response to improved irrigation use efficiency. *Sci. Rep.* **2020**, *10*, 1–15. [CrossRef] [PubMed]

53. Malakar, P.; Mukherjee, A.; Bhanja, S.N.; Saha, D.; Ray, R.K.; Sarkar, S.; Zahid, A. Importance of spatial and depth-dependent drivers in groundwater level modeling through machine learning. *Hydrol. Earth Syst. Sci. Discuss.* **2020**, *2020*, 1–22.

54. Water Resources Department, Directorate of Irrigation Research & Development. *Laboratory Testing Procedure for Soil & Water Sample Analysis*; Directorate of Irrigation Research & Development: Pune, India, 2009.

55. R Core Team. *R: A Language and Environment for Statistical Computing*; R Foundation for Statistical Computing: Vienna, Austria, 2018.

56. Searle, S.; Speed, F.; Milliken, G. Population Marginal Means in the Linear Model: An Alternative to Least Squares Means. *Am. Stat.* **1980**, *34*, 216–221. [CrossRef]

57. Lenth, R.V. Least-Squares Means: The R PackageIsmeans. *J. Stat. Softw.* **2016**, *69*, 1–33. [CrossRef]

58. Terink, W.; Khanal, S. *SPHY, Spatial Processes in Hydrology. Advanced Training, Input Data, Sensitivity Analysis, Model Calibration, and Scenario Analyses*; FutureWater: Wageningen, The Netherlands, 2016.

59. Terink, W.; Terink, W.; Lutz, A.F.; Simons, G.W.H.; Immerzeel, W.W.; Droogers, P. Sphy V2.0. *Spat. Process. Hydrol. Geosci. Model. Dev.* **2015**, *8*, 2009–2034. [CrossRef]

60. Kennedy, J.; Eberhart, R. Particle Swarm Optimization. In Proceedings of the IEEE International Conference on Neural Networks, Perth, WA, Australia, 27 November–1 December 1995; IEEE: New York, NY, USA, 1995.

61. Saxton, K.E.; Rawls, W.; Romberger, J.S.; Papendick, R.I. Estimating Generalized Soil-water Characteristics from Texture. *Soil Sci. Soc. Am. J.* **1986**, *50*, 1031–1036. [CrossRef]

62. Baccini, A.; Walker, W.; Carvalho, L.; Farina, M.; Sulla-Menashe, D.; Houghton, R.A. Tropical forests are a net carbon source based on aboveground measurements of gain and loss. *Science* **2017**, *358*, 230–234. [CrossRef] [PubMed]

63. Lehner, B.; Verdin, K.; Jarvis, A. New Global Hydrography Derived from Spaceborne Elevation Data. *EosTrans. Am. Geophys. Union* **2011**, *89*, 93–94. [CrossRef]

64. Horn, B. Hill shading and the reflectance map. *Proc. IEEE* **1981**, *69*, 14–47. [CrossRef]

65. O'Callaghan, J.F.; Mark, D.M. Extraction of Drainage Networks from Digital Elevation Data. *Comput. Vis. Graph. Image Process.* **1984**, *28*, 328–344. [CrossRef]

66. Barnes, R. RichDEM: Terrain Analysis Software. Available online: http://github.com/r-barnes/richdem (accessed on 31 March 2021).

67. Hengl, T.; De Jesus, J.M.; Heuvelink, G.B.M.; Gonzalez, M.R.; Kilibarda, M.; Blagotić, A.; Shangguan, W.; Wright, M.N.; Geng, X.; Bauer-Marschallinger, B.; et al. SoilGrids250m: Global gridded soil information based on machine learning. *PLoS ONE* **2017**, *12*, e0169748. [CrossRef]

68. Campbell, G.S.; Shiozawa, S. Prediction of Hydraulic Properties of Soils Using Particle-Size Distribution and Bulk Density Data. In Proceedings of the International Workshop on Indirect Methods for Estimating the Hydraulic Properties of Unsaturated Soils, Riverside, CA, USA, 11–13 October 1989; pp. 317–329.

69. Cosby, B.J.; Hornberger, G.M.; Clapp, R.B.; Ginn, T. A Statistical Exploration of the Relationships of Soil Moisture Characteristics to the Physical Properties of Soils. *Water Resour. Res.* **1984**, *20*, 682–690. [CrossRef]

70. Jabro, J.D. Estimation of Saturated Hydraulic Conductivity of Soils from Particle Size Distribution and Bulk Density Data. *Trans. ASAE* **1992**, *35*, 557–560. [CrossRef]

71. Puckett, W.E.; Dane, J.H.; Hajek, B.F. Physical and Mineralogical Data to Determine Soil Hydraulic Properties. *Soil Sci. Soc. Am. J.* **1985**, *49*, 831–836. [CrossRef]

72. Dane, J.H.; Puckett, E.W.; Hajek, B.F. Field Soil Hydraulic Properties Based on Physical and Mineralogical Information. In Proceedings of the International Workshop on Indirect Methods for Estimating the Hydraulic Properties of Unsaturated Soils, Riverside, CA, USA, 11–13 October 1989; pp. 389–403.

73. Chakraborty, D.; Mazumdar, S.P.; Garg, R.N.; Banerjee, S.; Santra, P.; Singh, R.; Tomar, R.K. Pedotransfer functions for predicting points on the moisture retention curve of Indian soils. *Indian J. Agric. Sci.* **2011**, *81I*, 1031.

74. Chakraborty, D.; Chakraborty, A.; Santra, P.; Tomar, R.K.; Garg, R.N.; Sahoo, R.N.; Choudhury, S.G.; Bhavanarayana, M.; Kalra, N. Prediction of hydraulic conductivity of soils from particle-size distribution. *Curr. Sci.* **2006**, *90*, 1526–1531.

75. Gupta, S.C.; Larson, W.E. Estimating soil water retention characteristics from particle size distribution, organic matter percent, and bulk density. *Water Resour. Res.* **1979**, *15*, 1633–1635. [CrossRef]

76. Rawls, W.J.; Brakensiek, D.L.; Miller, N. Green-ampt Infiltration Parameters from Soils Data. *J. Hydraul. Eng.* **1983**, *109*, 62–70. [CrossRef]

77. Tomasella, J.; Hodnett, M.G. Estimating Soil Water Retention Characteristics from Limited Data in Brazilian Amazonia. *Soil Sci.* **1998**, *163*, 190–202. [CrossRef]

78. Hodnett, M.G.; Tomasella, J. Marked differences between van Genuchten soil water-retention parameters for temperate and tropical soils, a new water-retention pedo-transfer functions developed for tropical soils. *Geoderma* **2002**, *108*, 155–180. [CrossRef]

79. Varallyay, G.; Rajkai, K.; Pachepsky, Y.A.; Shcherbakov, R.A. Mathematical description of soil water retention curve. *Pochvovedenie* **1982**, *4*, 77–89.

80. Wösten, J.; Lilly, A.; Nemes, A.; Le Bas, C. Development and use of a database of hydraulic properties of European soils. *Geoderma* **1999**, *90*, 169–185. [CrossRef]

81. Vereecken, H.; Maes, J.; Feyen, J.; Darius, P. Estimating the soil moisture retention characteristic from texture, bulk density, and carbon content. *Soil Sci.* **1989**, *148*, 389–403. [CrossRef]

82. Running, S.; Mu, Q.; Zhao, M. MOD16A2 MODIS/Terra Net Evapotranspiration 8-Day L4 Global 500 m SIN Grid V006 [Data Set]. Available online: https://lpdaac.usgs.gov/products/mod16a2v006/ (accessed on 31 March 2021).

83. Myneni, R.; Knyazikhin, Y.; Park, T. MOD15A2H MODIS/Terra Leaf Area Index/FPAR 8-Day L4 Global 500 m SIN Grid V006. Available online: https://lpdaac.usgs.gov/products/mod15a2hv006/ (accessed on 31 March 2021).

84. Hong, Y.; Gochis, D.; Cheng, J.-T.; Hsu, K.-L.; Sorooshian, S. Evaluation of PERSIANN-CCS Rainfall Measurement Using the NAME Event Rain Gauge Network. *J. Hydrometeorol.* **2007**, *8*, 469–482. [CrossRef]

85. Mahrooghy, M.; Anantharaj, V.G.; Younan, N.H.; Aanstoos, J.; Hsu, K.-L. On an Enhanced PERSIANN-CCS Algorithm for Precipitation Estimation. *J. Atmos. Ocean. Technol.* **2012**, *29*, 922–932. [CrossRef]

86. Bosch, J.M.; Hewlett, J.D. A review of catchment experiments to determine the effect of vegetation changes on water yield and evapotranspiration. *J. Hydrol.* **1982**, *55*, 3–23. [CrossRef]

87. Robinson, M.; Cognard-Plancq, A.-L.; Cosandey, C.; David, J.; Durand, P.; Führer, H.-W.; Hall, R.; Hendriques, M.; Marc, V.; McCarthy, R.; et al. Studies of the impact of forests on peak flows and baseflows: A European perspective. *Ecol. Manag.* **2003**, *186*, 85–97. [CrossRef]

88. Van Noordwijk, M.; Tanika, L.; Lusiana, B. Flood risk reduction and flow buffering as ecosystem services—Part 1, Theory on flow persistence, flashiness and base flow. *Hydrol. Earth Syst Sci.* **2017**, *21*, 2321–2340. [CrossRef]

89. Van Noordwijk, M. Agroforestry as part of climate change response; IOP Conference Series. *Earth Environ. Sci.* **2018**, *200*, 012002.

90. Paul, S.; Ghosh, S.; Rajendran, K.; Murtugudde, R. Moisture Supply from the Western Ghats Forests to Water Deficit East Coast of India. *Geophys. Res. Lett.* **2018**, *45*, 4337–4344. [CrossRef]

91. Agus, F.; Irawan, I.; Suganda, H.; Wahyunto, W.; Setiyanto, A.; Kundarto, M. Environmental multifunctionality of Indonesian agriculture. *Paddy Water Environ.* **2006**, *4*, 181–188. [CrossRef]

92. Wangpakapattanawong, P.; Finlayson, R.; Öborn, I.; Roshetko, J.M.; Sinclair, F.; Shono, K.; Borelli, S.; Hillbrand, A.; Conigliaro, M. Agroforestry in Rice-Production Landscapes in Southeast Asia: A Practical Manual. Available online: http://www.fao.org/3/i7137e/i7137e.pdf (accessed on 31 March 2021).

93. Spracklen, D.V.; Arnold, S.R.; Taylor, C.M. Observations of increased tropical rainfall preceded by air passage over forests. *Nature* **2012**, *489*, 282–285. [CrossRef]

94. Davis, K.F.; Chiarelli, D.D.; Rulli, M.C.; Chhatre, A.; Richter, B.; Singh, D.; DeFries, R. Alternative cereals can improve water use and nutrient supply in India. *Sci. Adv.* **2018**, *4*, 1108. [CrossRef] [PubMed]

95. Pandey, D.N. Multifunctional agroforestry systems in India. *Curr. Sci.* **2007**, *92*, 455–463.

96. Viswanath, S.; Lubina, P.A.; Subbanna, S.; Sandhya, M.C. Traditional Agroforestry systems and practices. A review. *Adv. Agric. Res. Technol.* **2018**, *2*, 18–19.

97. Chinnamani, S. Agroforestry research in India: A brief review. *Agrofor. Syst.* **1993**, *23*, 253–259. [CrossRef]

98. Santoro, A.; Venturi, M.; Bertani, R.; Agnoletti, M. A Review of the Role of Forests and Agroforestry Systems in the FAO Globally Important Agricultural Heritage Systems (GIAHS) Programme. *Forests* **2020**, *11*, 860. [CrossRef]